Biochemical and Biophysical Research Communications 450 (2014) 49–54

Contents lists available at ScienceDirect

Biochemical and Biophysical Research Communications

journal homepage: www.elsevier.com/locate/ybbrc

Identification of a novel multiple kinase inhibitor with potent antiviral activity against influenza virus by reducing viral polymerase activity

Yutaka Sasaki [a,1], Michinori Kakisaka [a,1], Nopporn Chutiwitoonchai [a], Shigeru Tajima [b], Hirokazu Hikono [c], Takehiko Saito [c], Yoko Aida [a,*]

[a] Viral Infectious Diseases Unit, RIKEN, 2-1 Hirosawa, Wako, Saitama 351-0198, Japan
[b] Department of Virology I, National Institute of Infectious Diseases, 1-23-1 Toyama, Shinjuku, Tokyo 162-8640, Japan
[c] Influenza and Prion Disease Research Center, National Institute of Animal Health, National Agriculture and Food Research Organization (NARO), 3-1-5 Kannondai, Tsukuba, Ibaraki 305-0856, Japan

ARTICLE INFO

Article history:
Received 30 April 2014
Available online 22 May 2014

Keywords:
Anti-influenza viral drug
Compound library screening
vRNP activity
Kinase inhibitor
Target database search
KINOMEscan

ABSTRACT

Neuraminidase inhibitors are the only currently available influenza treatment, although resistant viruses to these drugs have already been reported. Thus, new antiviral drugs with novel mechanisms of action are urgently required. In this study, we identified a novel antiviral compound, WV970, through cell-based screening of a 50,000 compound library and subsequent lead optimization. This compound exhibited potent antiviral activity with nanomolar IC_{50} values against both influenza A and B viruses but not non-influenza RNA viruses. Time-of-addition and indirect immunofluorescence assays indicated that WV970 acted at an early stage of the influenza life cycle, but likely after nuclear entry of viral ribonucleoprotein (vRNP). Further analyses of viral RNA expression and viral polymerase activity indicated that WV970 inhibited vRNP-mediated viral genome replication and transcription. Finally, structure-based virtual screening and comprehensive human kinome screening were used to demonstrate that WV970 acts as a multiple kinase inhibitor, many of which are associated with influenza virus replication. Collectively, these results strongly suggest that WV970 is a promising anti-influenza drug candidate and that several kinases associated with viral replication are promising drug targets.

1. Introduction

Seasonal influenza infection causes large scale economic burdens, and pandemics such as those caused by the highly pathogenic avian influenza A subtypes, including H5N1 and H7N7 could result in millions of deaths [1,2]. Thus, anti-influenza drugs have been developed for prevention and treatment of influenza infections. Two classes of anti-influenza drugs are currently approved for clinical use, M2 channel blockers and neuraminidase (NA) inhibitors [3]. However, the clinical uses of M2 channel blockers are limited since all currently circulating influenza A virus strains are resistant to these drugs [4]. Moreover, the emergence of NA inhibitor-resistant viruses has also been reported [4,5]. If NA inhibitor-resistant viruses become more widespread then there will be few effective means of treating influenza infections. Therefore, new antivirals based on novel mechanisms of action are urgently needed.

One potential approach is to target host factors involved in influenza replication, which may provide a novel antiviral strategy to counteract viral drug resistance. Recent reports revealed that a large number of host factors are involved in influenza replication and that the majority of these are kinases [6]. Indeed, several kinase inhibitors including Ca^{2+}/calmodulin-dependent protein kinase (CAMK), protein kinase C (PKC), phosphoinositide 3-kinase (PI3K), receptor tyrosine kinases (RTKs) and MAPK/ERK kinase (MEK) exhibit potent anti-influenza activity [7].

Structure-based virtual screening is one of the most convenient and promising approaches for identifying potential binding partners for test compounds, and can provide targets that have a high likelihood of binding to the query compound [8]. In addition, a comprehensive human kinome screening system (KINOMEscan) was used to provide quantitative data on binding selectivity between test compounds and more than 450 human kinases [9]. In this study, we identified a novel antiviral compound, WV970, using a cell-based influenza A infection assay and optimized the compound by assessing structure–activity relationships (SAR). The mechanism of action was further characterized, wherein WV970 behaved as a multiple kinase inhibitor.

* Corresponding author. Fax: +81 48 462 4399.
E-mail address: aida@riken.jp (Y. Aida).
[1] Equal contributors.

http://dx.doi.org/10.1016/j.bbrc.2014.05.058
0006-291X/

2. Materials and methods

2.1. Compounds

The chemical library for cell-based screening was purchased from ChemBridge, and hit compound RK188 was purchased from Sundia MediTech. WV635 and WV970 were synthesized by Wakunaga Pharmaceuticals and a stock solution of 10 mM was prepared in dimethyl sulfoxide (DMSO). Oseltamivir carboxylate and nucleozin were purchased from Kemprotec and Shanghai Haoyuan Chemexpress, respectively.

2.2. Cells and viruses

Madin-Darby canine kidney (MDCK) cells, Vero cells and HEK293T cells were grown in Dulbecco's modified Eagle's medium (DMEM, Invitrogen) containing penicillin, streptomycin, and glutamine (PSG, GIBCO Industries Inc.) and 10% fetal bovine serum (Sigma–Aldrich). Influenza A viruses, including A/WSN/1933 (H1N1), A/Udorn/307/1972 (H3N2), A/ck/Yamaguchi/7/2004 (H5N1), and A/Anhui/1/2013 (H7N9), and influenza B viruses, including B/Yamagata/16/88 and B/Nagasaki/1/87, were propagated in MDCK cells. Japanese encephalitis virus (JEV) (Mie/41/2002 strain) and dengue virus type I (NIID 02-20) were propagated in Vero cells.

2.3. Random screening of compounds with MDCK cell-based influenza A infection assays

MDCK cells (3×10^4 cells/well) were seeded in 96-well plates and incubated at 37 °C in 5% CO_2 overnight with DMEM containing 10 μM library compounds, and then inoculated with influenza A virus (A/WSN/1933) at a multiplicity of infection (MOI) of 0.005 with 1 μg/ml of tosylsulfonyl phenylalanyl chloromethyl ketone-treated trypsin (Trypsin-TPCK, Worthington Biochemical Corporation). After a 48 h incubation, the cells were washed twice with phosphate-buffered saline (PBS), and 10 μl of WST-1 reagent (Takara Bio) was added into each well. The plate was incubated at 37 °C for 1 h, and absorbance was measured at 450 nm. Inhibition (%) of virus-induced cytopathic effects (CPEs) was evaluated by comparing test compound-treated cells to DMSO-treated cells.

2.4. Plaque assays of antiviral activity

Plaque assays for influenza viruses were performed as previously described [10]. For plaque assays with JEV and dengue virus, Vero cells (6×10^5 cells/well) were seeded in 6-well plates and incubated at 37 °C in 5% CO_2 for 24 h. Cells were washed once with PBS and inoculated with approximately 200 plaque forming units (PFU) of JEV or dengue virus. After incubating for 1 h at 37 °C in 5% CO_2, 2 ml of DMEM containing 1% methylcellulose was overlaid onto each well. Cells were incubated at 37 °C in 5% CO_2 for 5 days after JEV inoculation or 7 days after dengue virus inoculation. After the removal of DMEM containing methylcellulose, cells were fixed with 3.7% formaldehyde and stained with 0.1% crystal violet. The 50% inhibitory concentration (IC_{50}) was then evaluated by counting the number of plaques.

2.5. Cell toxicity

Cell toxicity was measured as previously described [10] using a WST-1 assay. The 50% cytotoxic concentration (CC_{50}) was evaluated by comparing test compound-treated cells to DMSO-treated cells.

2.6. Indirect immunofluorescence

Indirect immunofluorescence was performed as described previously [11] with a primary anti-NP monoclonal antibody (MAb) (Santa Cruz Biotechnology) and subsequent secondary Alexa Fluor 488-conjugated rabbit anti-mouse IgG (Invitrogen). Samples were then incubated with PBS containing Hoechst 33342 (Immuno-Chemistry Technologies LLC) for nuclear staining. Prepared samples were observed under a confocal laser-scanning microscope (FV 1000, Olympus).

2.7. RNA fluorescence in situ hybridization (FISH) analysis

RNA FISH was performed according to published protocols [12]. Probes targeting the PB2 segment of the influenza virus were designed by Stellaris RNA FISH Probe Designer and purchased from Biosearch Technologies. Prepared samples were observed under a confocal laser-scanning microscope (FV 1000, Olympus).

2.8. Real-time quantitative reverse transcription-polymerase chain reaction (qRT-PCR)

RNA was extracted from MDCK cells (1.2×10^6 cells/well) infected with A/WSN/1933 at an MOI of 10 using TRIzol® LS Reagent (Invitrogen).

RT-PCR was performed using SuperScript™ III First-Strand Synthesis System (Invitrogen) according to the manufacturer's instructions and specific primers for the following three targets using a previously described protocol [13]: viral genome RNA (vRNA) NP (F), 5′-GGCCGTCATGGTGGCGAATGAATGGACGGAGAACAAGGATTGC-3′; viral mRNA NP (R), 5′-CCAGATCGTTCGAGTCGTTTTTTTTTTTTTTTTCTTTAATTGTC-3′; and mRNA MDCK actin (R), 5′-GGAACCGCTCGTTGCCAATG-3′.

For qPCR, each cDNA was used with 2 × SYBR GreenER qPCR SuperMix (Invitrogen) and ABI PRISM, according to the manufacturer's instructions. The specific primers used are as follows: vRNA NP (F), 5′-GGCCGTCATGGTGGCGAAT-3′; vRNA NP (R), 5′-CTCAATATGAGTGCAGACCGTGCT-3′; viral mRNA NP (F), 5′-CGATCGTGCCCTCCTTTG-3′; viral mRNA NP (R), 5′-CCAGATCGTTCGAGTCGT-3′; mRNA MDCK actin (F), 5′-CGTGCGTGACATCAAGGAAGAAG-3′; and mRNA MDCK actin (R), 5′-GGAACCGCTCGTTGCCAATG-3′. Data were analyzed using the ΔΔCT method. MDCK actin was used as a control.

2.9. Mini-genome assays

Mini-genome assays were performed using the expression plasmids PB1/pCAGGS, PB2/pCAGGS, PA/pCAGGS, NP/pCAGGS and vNP-luc/pHH21, as described previously [10].

2.10. Western blot analysis

Western blot analysis was performed with an anti-WSN polyclonal antibody (Ab) and HRP-conjugated goat anti-rabbit IgG (Amersham Bioscience) or anti-β-actin MAb (Sigma–Aldrich) and HRP-conjugated goat anti-mouse IgG (Amersham Bioscience), as described previously [11].

2.11. LASSO (ligand activity by surface similarity order) screening with the ChemSpider database

Target molecule searches using the structure-based virtual screening database, ChemSpider (Royal Society of Chemistry), were conducted to identify potential binding partners for test compounds. LASSO scores ranges from 0 to 1.0, where a score of

0 represents a likely absence of binding and 1.0 represents the highest likelihood of binding to the target molecule [8].

2.12. KINOMEscan

KINOMEscan (DiscoveRx) employs a competition binding assay to quantitatively measure interactions between a test compound and more than 450 human kinases [9]. After the competition reaction, the amount of kinase bound to the immobilized ligand is determined using quantitative PCR of a DNA tag conjugated to the kinase. Data are represented as a percentage of control (% Ctrl) where 100% indicates that the test compound did not inhibit kinase activity and lower numbers indicate stronger hits. KINOMEscan technology was used to screen WV970 (50 nM) against 456 kinases according to the protocol above.

3. Results

3.1. Screening of antiviral compounds and identification of WV970

To identify novel compounds targeting the influenza virus, we screened 50,000 compounds using an MDCK cell-based influenza infection assay. This assay identifies compounds according to their ability to protect against influenza virus-induced CPEs. Forty-seven primary hits were identified. Plaque assays were then used as a secondary screen to evaluate the IC_{50} of these compounds. Four hit compounds showed an $IC_{50} \leqslant 3$ μM in the plaque assays. Notably, RK188 was a racemic mixture (with an IC_{50} of 2.2 ± 0.25 μM) resulting from two chiral carbons at the C_7 and C_{14} positions (Fig. 1A). Next, we evaluated four compounds with different configurations ('*R*' or '*S*') that were stereoselectively synthesized at the C_7 and C_{14} positions of RK188. Among the four stereoisomers, WV635, which has the '*S*' configuration at both the C_7 and C_{14} positions, exhibited the most potent antiviral activity with an IC_{50} of 0.53 ± 0.05 μM against the A/WSN/1933 strain. Based on a SAR study of the lead compound WV635, we obtained WV970. This compound was the most potent (with an IC_{50} of 0.015 ± 0.060 μM) of approximately 160 derivatives that were evaluated against the A/WSN/1933 strain. Its antiviral activity was similar to that of oseltamivir carboxylate (IC_{50} = 0.012 ± 0.004 μM), which is a currently available antiviral drug, and its cytotoxic effects were lower than its antiviral effects (CC_{50} = 3.8 ± 4.5 μM, SI = 253.3). Moreover, WV970 exhibited potent antiviral activity against seasonal viral strains, including influenza A strain, A/Udorn/307/1972 (H3N2) and influenza B strains, B/Yamagata/16/88 and B/Nagasaki/1/87, in addition to the highly pathogenic avian influenza viral strains A/ck/Yamaguchi/7/2004 (H5N1) and A/Anhui/1/2013 (H7N9) (Fig. 1B). Interestingly, WV970 had no antiviral effects against non-influenza RNA viruses, such as JEV and dengue virus (Fig. 1 B), suggesting that WV970 may target an influenza virus-specific replication mechanism.

3.2. WV970 acts at an early stage of the viral life cycle

To determine the mechanisms by which WV970 acts during the influenza virus life cycle, a time-of-addition experiment was conducted following the scheme illustrated in Fig. 2A upper panel. WV970 inhibited viral production by up to approximately 20–50% when added to infected cells at an early time point (up to 4 h post-infection; Fig. 2A, lower panel). By contrast, WV970 had no

A

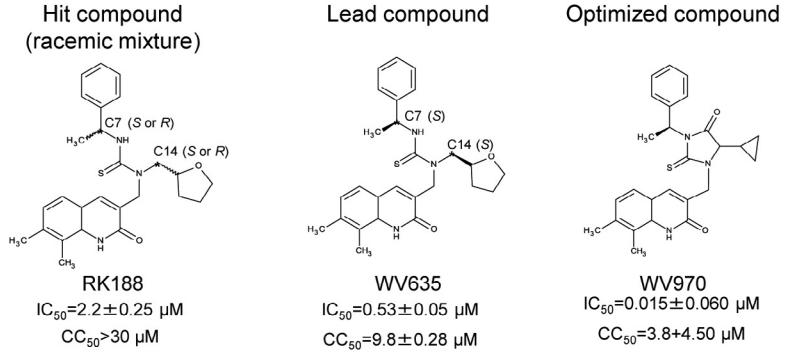

B

Host cell or Virus strain	WV970 CC_{50} (μM)	WV970 IC_{50} (μM)	WV970 SI	Oseltamivir carboxylate CC_{50} (μM)	Oseltamivir carboxylate IC_{50} (μM)
MDCK	3.8±4.5	-	-	>30	-
A/WSN/1933(H1N1)	-	0.015±0.060	253.3	-	0.012±0.004
A/Udorn/307/1972 (H3N2)	-	0.024±0.031	158.3	-	-
A/Ck/yamaguchi /7/2004(H5N1)	-	0.240±0.100	15.8	-	0.570±0.040
A/Anhui/1/2013(H7N9)	-	0.230±0.180	16.5	-	0.600±0.120
B/Yamagata/16/88	-	0.058±0.014	65.5	-	0.098±0.003
B/Nagasaki/1/87	-	0.020±0.030	190.0	-	0.019±0.004
Japanese encephalitis virus Mie/41/2002 strain	-	>30	-	-	-
Dengue virus type 1 NID 02-20 strain	-	>30	-	-	-

Fig. 1. The effect of WV970 on viral replication and cell viability. (A) Chemical structures of hit, lead and optimized compounds and their 50% inhibitory concentration (IC_{50}) against influenza A/WSN/1933 (H1N1) virus and 50% cytotoxic concentration (CC_{50}) against MDCK cells. (B) IC_{50} and CC_{50} values of WV970 and oseltamivir carboxylate against the indicated influenza A and B virus strains, non-influenza viruses or cell line. The IC_{50} of each compound was evaluated by plaque assay and the CC_{50} of each compound was evaluated by WST-1 assay in the absence or presence of the test compound (0–30 μM). Oseltamivir carboxylate was used as a positive control. Values represent the mean ± SD of three independent experiments. A Selectivity Index (SI) was calculated from the CC_{50} to IC_{50} ratio. (–) not tested.

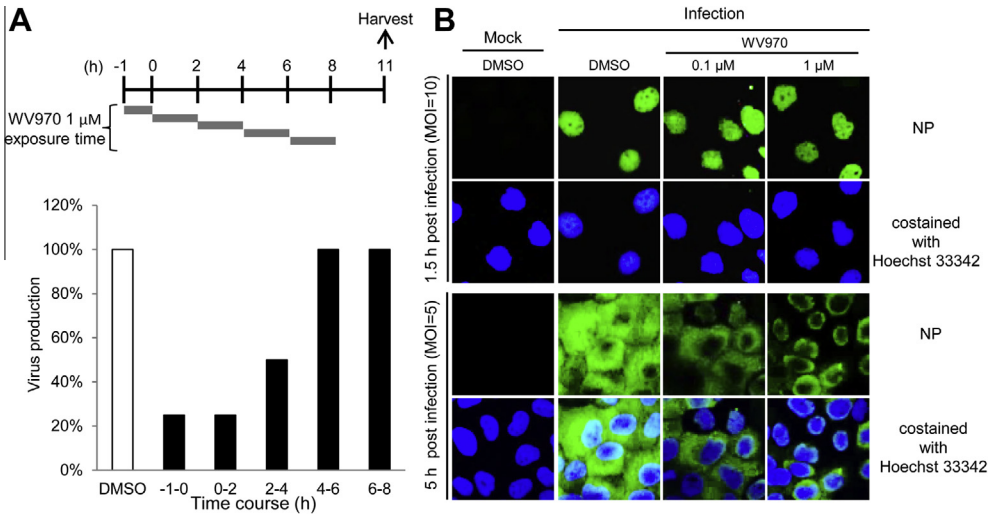

Fig. 2. Stage of the viral life cycle targeted by WV970. (A) WV970 was added at the indicated time points into MDCK cells preliminarily inoculated with A/WSN/1933 viruses at a multiplicity of infection (MOI) of 1 and cell supernatants were collected 11 h post-infection. The viral titer of collected supernatants was estimated by the hemagglutinin (HA) assay. (B) MDCK cells were infected with A/WSN/1933 at an MOI of 10 for 1.5 h, or MOI of 5 for 5 h in the absence or presence of WV970. Immunofluorescence staining was performed with an anti-NP monoclonal antibody (MAb) followed by anti-mouse Alexa Fluor 488 and Hoechst 333342. Cells were then observed under a confocal laser-scanning microscope.

inhibitory effects on viral production when added 4 h post-infection or later. This indicates that WV970 acts at an early stage of influenza virus life cycle unlike the oseltamivir carboxylate that inhibits the late step of the life cycle by blocking viral NA activity.

To further examine this hypothesis, we first explored the effect of WV970 on the nuclear entry of NP, which is the major component of viral ribonucleoprotein (vRNP: the complex with one copy of vRNA and a trimeric RNA polymerase (PB1, PB2 and PA) and multiple copies of NP) and can be detected in the nucleus of infected cells within 1 h post-infection [14]. At 1.5 h post-infection, NP accumulated in the nucleus and no differences were observed in DMSO- and WV970-treated cells, indicating that WV970 might act at a later stage than nuclear entry (Fig. 2B, upper panel). Next, we examined NP localization at 5 h post-infection when viral replication and transcription has begun and the vRNP reconstructed by newly synthesized viral proteins is exported to cytoplasm from the nucleus [15]. In DMSO-treated cells, NP was localized predominantly in the cytoplasm, with lesser amounts in the nucleus. Interestingly, in WV970-treated cells, NP was observed in the cytoplasm but expression levels decreased dose-dependently (Fig. 2B, lower panel). These results suggest that WV970 might inhibit vRNP activity, which regulates viral genome replication and transcription.

3.3. WV970-mediated inhibition of the viral genome replication, transcription and protein expression

To examine the effects of WV970 on vRNP activity, we performed FISH analysis using Cy5-labeled DNA oligos targeted against vRNA encoding the PB2 protein (Fig. 3A). In DMSO-treated cells, vRNA expression increased in the nucleus and cytoplasm of infected cells in a time-dependent manner. By contrast, a significant decrease in vRNA expression was observed in WV970-treated cells.

To examine whether WV970 also affects viral genome transcription, we assessed vRNA and viral mRNA expression levels by qRT-PCR analysis. In WV970-treated cells, vRNA and mRNA expression levels were significantly lower (at both 5 h and 10 h post-infection) than those of DMSO-treated cells. Similar results were obtained with nucleozin-treated cells, as nucleozin is an NP inhibitor used as a positive control for blocking of viral transcription and replication [16]. By contrast, oseltamivir carboxylate had no significant effect (Fig. 3B).

To further investigate whether WV970 inhibits vRNP activity, we conducted a mini-genome assay using four viral protein expression plasmids (pCAGGS) encoding PB1, PB2, PA and NP, and the viral-like genome expression plasmid NP-luc/pPolI encoding firefly luciferase. WV970, but not oseltamivir carboxylate or DMSO, decreased luciferase activity in a dose-dependent manner (Fig. 3C).

Finally, we examined the effect of WV970 on the subsequent viral protein expression (Fig. 3D). Western blot analysis showed that WV970 inhibited expression of HA, NP, NA and M1 when compared to that of oseltamivir carboxylate and DMSO.

Collectively, these results indicate that WV970 inhibits vRNP-mediated viral genome replication and transcription.

3.4. Target protein searches and comprehensive kinome screening for WV970

Since we could not isolate WV970 resistant viruses after several passages of viral propagation under selection pressure for WV970 (data not shown), we hypothesized that WV970 may be involved in the inhibition of an essential host factor for virus replication and not viral components per se. Thus, we conducted a target search with a structure-based virtual screening database [8] and several kinase molecules were identified with high LASSO scores when the chemical structure of WV635 was used as a query. These results suggest that WV970, which is a derivative compound of WV635, may also target a kinase even though no target molecules were identified with WV970 (Fig. 4A). To confirm this hypothesis, we examined the effect of WV970 on kinase inhibition. It is well known that most kinase inhibitors interact with a wide range of kinases with different activities [17]. To examine the binding affinity of WV970 against a large number of kinases, we conducted KINOMEscan screening, which is based on an ATP site competition binding assay [9]. WV970 was screened at a concentration of 50 nM against 456 kinases, covering more than 80% of human protein kinases. WV970 exhibited inhibitory effects (lower than 50% of Ctrl, which indicates a greater than 50% displacement from an immobilized target kinase) against only 15 kinases. These results are consistent with the hypothesis above (based on the

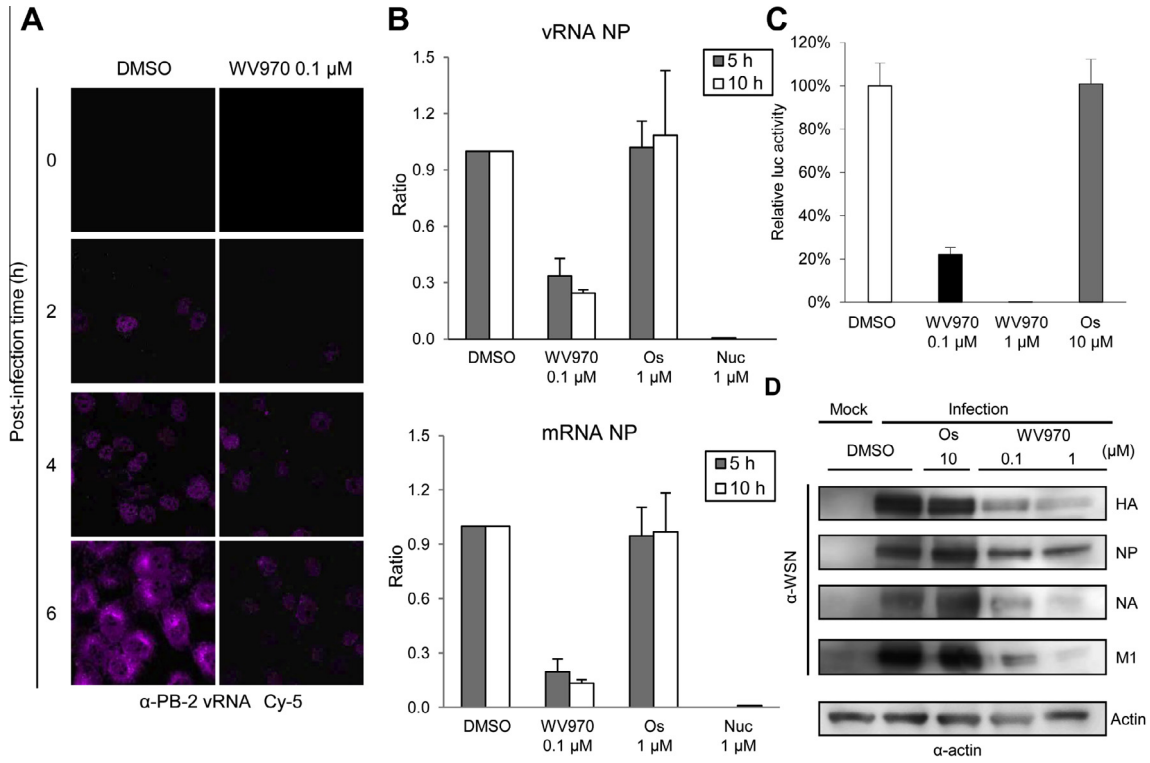

Fig. 3. Effects of WV970 on viral transcription, replication and protein expression. (A) MDCK cells were infected with A/WSN/1933 virus at an MOI of 5 in the absence or presence of 0.1 μM WV970, and fixed at 0, 2, 4 and 6 h post-infection. Cells were probed for PB2 vRNA using Cy5-labeled probes targeting the PB2 segment and then observed under a confocal laser-scanning microscope. (B) MDCK cells were infected with A/WSN/33 virus at an MOI of 10 in the absence or presence of test compounds. Os and Nuc represent oseltamivir carboxylate and nucleozin, respectively. After 5 h or 10 h post-infection, cell lysates were harvested and qRT-PCR was performed to detect NP vRNA and NP mRNA. The ratio of gene expression to its respective internal control (actin) was normalized to the control (DMSO) sample. Values represent the mean ± SD of three independent experiments. (C) HEK-293T cells were transfected with pCAGGS encoding PB1, PB2, PA and NP, and the viral-like genome expression plasmid, NP-luc/pol, in the absence or presence of test compounds. After 48 h, relative luciferase activity was measured. Values represent the mean ± SD of three independent experiments. (D) MDCK cells were infected with A/WSN/1933 virus at a MOI of 10 in the absence or presence of test compounds. Cell lysates were harvested 18 h post-infection, and Western blot analysis was performed to detect viral protein expression using an anti-WSN polyclonal antibody (Ab) and an anti- β -actin MAb. NP, HA, M1, and M2 proteins are shown. β-actin was used as a loading control.

structure-based virtual screening) that WV970 may target a kinase and indicate that WV970 acts as a multiple kinase inhibitor with a potent antiviral activity.

4. Discussion

In this study, we identified a novel anti-influenza compound, WV970, that inhibited RNP-mediated viral genome replication and transcription, thereby inhibiting viral replication of several influenza A and B virus strains, including the highly pathogenic avian influenza virus strains, A/ck/Yamaguchi/7/2004 (H5N1) and A/Anhui/1/2013 (H7N9). Further analyses, using structure-based virtual screening and comprehensive human kinome screening, revealed that WV970 selectively binds to 15 kinases. Several genome-wide RNAi screens have indicated that numerous host factors are required for influenza A virus replication and that the majority of these are kinases [6]. Previous reports demonstrate that various kinase inhibitors can suppress influenza A virus replication [7]. For example, PI3K inhibitors reduce influenza A virus replication by blocking vRNP activity [7]. In regard to our results, nine of the KINOMEscan hits have been reported to have the possibility of regulating influenza A virus replication [6]. Notably, five of these, DCLK1, EPHB2, JAK2, OXSR1 and HIPK2, have been reported to regulate the early stages of the influenza A virus life cycle, including viral genome replication and transcription [6]. In addition, some kinase inhibitors, such as MEK and PKC inhibitors interfere with both influenza A and B viruses [7]. Interestingly, WV970 did not exhibit antiviral effect against non-influenza RNA viruses. These findings indicate that WV970 may specifically inhibit viral genome replication and transcription of both influenza A and B viruses via inhibition of these kinase activities. However, to confirm this hypothesis, further investigations are required to define the detailed mechanisms by which these kinases regulate viral replication. Although the remaining six kinases identified, DSTYK, MAP3K1, SBK1, ULK1, IRAK4 and INSR, have not been reported to play a role in influenza replication [6], they may still influence this process, although further studies are required to confirm this possibility.

In addition to host factor effects, vRNP polymerase activity is regulated by its component viral proteins, including PB1, PB2, PA and NP. Apart from their fundamental protein functions such as cap-snatching and endonuclease activity [18], phosphoproteome analysis has demonstrated that phosphorylation of these proteins may also regulate viral replication, although the functional roles of this phosphorylation are not fully understood [19]. Notably, NP contains a number of potential phosphorylation sites, and phosphorylation of S165 is essential for genome replication and transcriptional activity [19], which indicates the importance of viral protein phosphorylation for vRNP activity. These results also strongly suggest that kinases play an essential role in influenza replication and that kinase inhibition is a promising drug target.

When targeting host factors as drug targets, drug-induced cytotoxic effects are a major concern because host functions may also be affected. However, viral polymerase activity was far more sensitive to WV970 than host factor activity, which thereby results

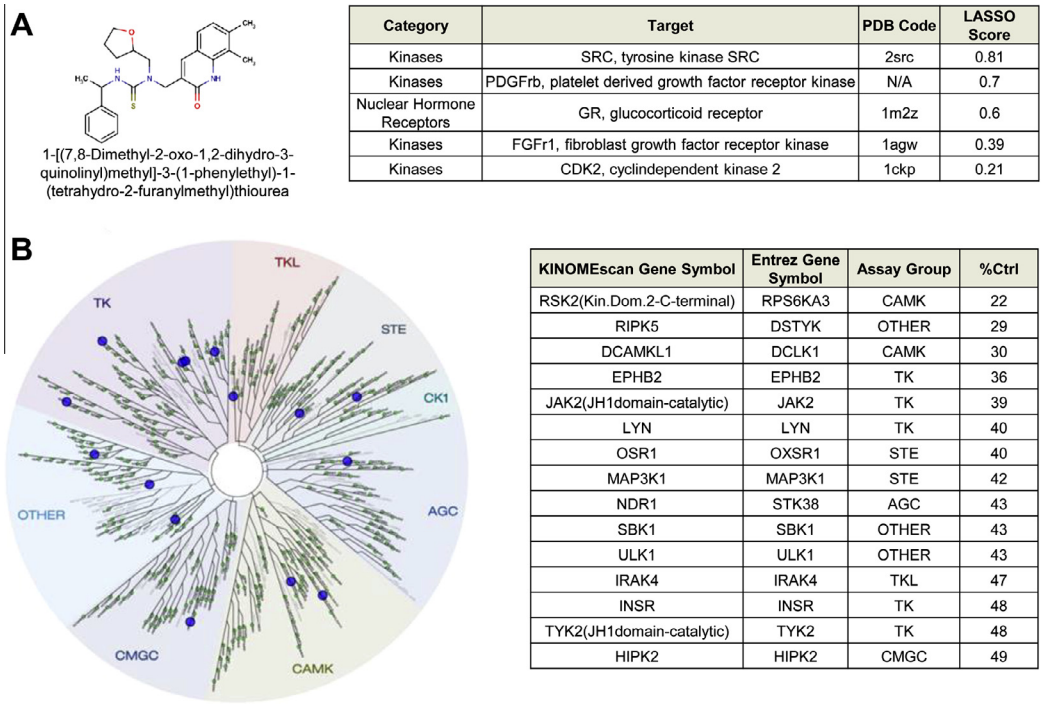

Category	Target	PDB Code	LASSO Score
Kinases	SRC, tyrosine kinase SRC	2src	0.81
Kinases	PDGFRb, platelet derived growth factor receptor kinase	N/A	0.7
Nuclear Hormone Receptors	GR, glucocorticoid receptor	1m2z	0.6
Kinases	FGFr1, fibroblast growth factor receptor kinase	1agw	0.39
Kinases	CDK2, cyclindependent kinase 2	1ckp	0.21

KINOMEscan Gene Symbol	Entrez Gene Symbol	Assay Group	%Ctrl
RSK2(Kin.Dom.2-C-terminal)	RPS6KA3	CAMK	22
RIPK5	DSTYK	OTHER	29
DCAMKL1	DCLK1	CAMK	30
EPHB2	EPHB2	TK	36
JAK2(JH1domain-catalytic)	JAK2	TK	39
LYN	LYN	TK	40
OSR1	OXSR1	STE	40
MAP3K1	MAP3K1	STE	42
NDR1	STK38	AGC	43
SBK1	SBK1	OTHER	43
ULK1	ULK1	OTHER	43
IRAK4	IRAK4	TKL	47
INSR	INSR	TK	48
TYK2(JH1domain-catalytic)	TYK2	TK	48
HIPK2	HIPK2	CMGC	49

Fig. 4. Target search for WV635 and the inhibitory effects of WV970 in a kinase library. (A) A target search was performed with the structure-based virtual screening database, ChemSpider, using the structure of the lead compound WV635 as a query. LASSO scores assessing the likelihood of the target (category and PDB code are shown) binding to the query compound are shown in the left panel. (B) Dendrogram (left panel) and table (right panel) of the human kinome demonstrating a kinase selectivity of 50 nM for WV970 against a panel of 456 human kinases (KINOMEscan gene symbol and enzyme gene symbol are listed in the table) including eight assay groups. Targets hit are colored blue in the dendrogram. The dendrogram was generated using TREEspot software with 50% control (% Ctrl) used as a cutoff.

in limited cytotoxicity. Thus, WV970 is a novel antiviral drug candidate with potential for further development.

In conclusion, WV970 acts as a multiple kinase inhibitor and exhibits potent antiviral effects against influenza virus through vRNP inhibition. Further studies are required to investigate the mechanisms of WV970-mediated inhibition of viral replication. Moreover, WV970 shows promise as a novel antiviral drug.

Acknowledgments

We thank Wakunaga Pharmaceuticals for kindly providing many compounds. We also thank Drs. Yoshihiro Kawaoka (University of Tokyo), Eri Nobusawa (National Institute of Infectious Diseases) and Kazufumi Shimizu (Nihon University) for kindly providing the plasmids used for the mini-genome assay, influenza B strains and anti-WSN antibody, respectively.

This study was supported in part by a RIKEN Program for Drug Discovery and Medical Technology Platforms, by the Adaptable and Seamless Technology Transfer Program through target-driven R&D (A-STEP) from Japan Science and Technology Agency (JST), and by a research project for improving food safety and animal health from the Ministry of Agriculture, Forestry and Fisheries of Japan.

References

[1] T.D. Szucs, Medical economics in the field of influenza – past, present and future, Virus Res. 103 (2004) 25–30.
[2] J.K. Taubenberger, J.C. Kash, Influenza virus evolution, host adaptation, and pandemic formation, Cell Host Microbe 7 (2010) 440–451.
[3] E. De Clercq, Antiviral agents active against influenza A viruses, Nat. Rev. Drug Discov. 5 (2006) 1015–1025.
[4] G.A. Poland, R.M. Jacobson, I.G. Ovsyannikova, Influenza virus resistance to antiviral agents: a plea for rational use, Clin. Infect. Dis. 48 (2009) 1254–1256.
[5] Y. Hu, S. Lu, Z. Song, W. Wang, P. Hao, J. Li, X. Zhang, H.L. Yen, B. Shi, T. Li, W. Guan, L. Xu, Y. Liu, S. Wang, X. Zhang, D. Tian, Z. Zhu, J. He, K. Huang, H. Chen, L. Zheng, X. Li, J. Ping, B. Kang, X. Xi, L. Zha, Y. Li, Z. Zhang, M. Peiris, Z. Yuan, Association between adverse clinical outcome in human disease caused by novel influenza A H7N9 virus and sustained viral shedding and emergence of antiviral resistance, Lancet 381 (2013) 2273–2279.
[6] T. Watanabe, S. Watanabe, Y. Kawaoka, Cellular networks involved in the influenza virus life cycle, Cell Host Microbe 7 (2010) 427–439.
[7] K.H. Muller, L. Kakkola, A.S. Nagaraj, A.V. Cheltsov, M. Anastasina, D.E. Kainov, Emerging cellular targets for influenza antiviral agents, Trends Pharmacol. Sci. 33 (2012) 89–99.
[8] ChemSpider database, <http://www.simbiosys.ca/ehits_lasso/LASSO_on_ChemSpider.pdf>.
[9] M.I. Davis, J.P. Hunt, S. Herrgard, P. Ciceri, L.M. Wodicka, G. Pallares, M. Hocker, D.K. Treiber, P.P. Zarrinkar, Comprehensive analysis of kinase inhibitor selectivity, Nat. Biotechnol. 29 (2011) 1046–1051.
[10] K. Yamada, H. Koyama, K. Hagiwara, A. Ueda, Y. Sasaki, S.N. Kanesashi, R. Ueno, H.K. Nakamura, K. Kuwata, K. Shimizu, M. Suzuki, Y. Aida, Identification of a novel compound with antiviral activity against influenza A virus depending on PA subunit of viral RNA polymerase, Microbes Infect. 14 (2012) 740–747.
[11] T. Murakami, Y. Aida, Visualizing Vpr-induced G2 arrest and apoptosis, PLoS One 9 (2014) e86840.
[12] Y.Y. Chou, N.S. Heaton, Q. Gao, P. Palese, R.H. Singer, T. Lionnet, Colocalization of different influenza viral RNA segments in the cytoplasm before viral budding as shown by single-molecule sensitivity FISH analysis, PLoS Pathog. 9 (2013) e1003358.
[13] E. Kawakami, T. Watanabe, K. Fujii, H. Goto, S. Watanabe, T. Noda, Y. Kawaoka, Strand-specific real-time RT-PCR for distinguishing influenza vRNA, cRNA, and mRNA, J. Virol. Methods 173 (2011) 1–6.
[14] C.N. Root, E.G. Wills, L.L. McNair, G.R. Whittaker, Entry of influenza viruses into cells is inhibited by a highly specific protein kinase C inhibitor, J. Gen. Virol. 81 (2000) 2697–2705.
[15] M.J. Amorim, E.A. Bruce, E.K. Read, A. Foeglein, R. Mahen, A.D. Stuart, P. Digard, A Rab11- and microtubule-dependent mechanism for cytoplasmic transport of influenza A virus viral RNA, J. Virol. 85 (2011) 4143–4156.
[16] R.Y. Kao, D. Yang, L.S. Lau, W.H. Tsui, L. Hu, J. Dai, M.P. Chan, C.M. Chan, P. Wang, B.J. Zheng, J. Sun, J.D. Huang, J. Madar, G. Chen, H. Chen, Y. Guan, K.Y. Yuen, Identification of influenza A nucleoprotein as an antiviral target, Nat. Biotechnol. 28 (2010) 600–605.
[17] S.P. Davies, H. Reddy, M. Caivano, P. Cohen, Specificity and mechanism of action of some commonly used protein kinase inhibitors, Biochem. J. 351 (2000) 95–105.
[18] A. York, E. Fodor, Biogenesis, assembly, and export of viral messenger ribonucleoproteins in the influenza A virus infected cell, RNA Biol. 10 (2013) 1274–1282.
[19] E.C. Hutchinson, E.M. Denham, B. Thomas, D.C. Trudgian, S.S. Hester, G. Ridlova, A. York, L. Turrell, E. Fodor, Mapping the phosphoproteome of influenza A and B viruses by mass spectrometry, PLoS Pathog. 8 (2012) e1002993.